Antiferromagnetic Materials

Deutsche Ausgabe: DOI: 10.1002/ange.201510576
Internationale Ausgabe: DOI: 10.1002/anie.201510576

β-Ag_3RuO_4, a Ruthenate(V) Featuring Spin Tetramers on a Two-Dimensional Trigonal Lattice

*Beluvalli E. Prasad, Pavel Kazin, Alexander C. Komarek, Claudia Felser, and Martin Jansen**

Dedicated to Professor Wolfgang Jeitschko on the occasion of his 80th Birthday

Abstract: *Open-shell solids exhibit a plethora of intriguing physical phenomena that arise from a complex interplay of charge, spin, orbital, and spin-state degrees of freedom. Comprehending these phenomena is an indispensable prerequisite for developing improved functional materials. This type of understanding can be achieved, on the one hand, by experimental and theoretical investigations into known systems, or by synthesizing new solids displaying unprecedented structural and/or electronic features.* β-Ag_3RuO_4 *may serve as such a model system because it possesses a remarkable anionic structure, consisting of tetrameric polyoxoanions* $(Ru_4O_{16})^{12-}$*, and is an embedded fragment of a 2D trigonal* MO_2 *lattice. The notorious frustration of antiferromagnetic (AF) exchange couplings on such lattices is thus lifted, and instead strong AF occurs within the oligomeric anion, where only one exchange path remains frustrated among the relevant six. The strong magnetic anisotropy of the* $[Ru_4O_{16}]^{12-}$ *ion, and the effectively orbital nature of its net magnetic moment, implies that this anion may reveal the properties of a single-molecule magnet if well-diluted in a diamagnetic matrix.*

Doubly negatively charged oxygen is unstable as a free ion, and thus it can only be incorporated into a chemical environment if particular mechanisms of stabilization are enabled. An external positive potential provided by surrounding cations in a prevailingly ionic crystal is one of the most obvious options.[1] Another process giving relief to excess electron density is catenation with homo-atomic bonds, forming peroxide, superoxide, or ozonide anions.[2] For high oxidation state oxide materials, electron transfer to the coordinated cations commonly occurs within some kind of covalent bonding. This feature of oxygen is one of the principal reasons for the tremendous wealth of structures and properties displayed by (multinary) oxides. Among others, classes of materials include top performing ferroelectrics,[3] ferromagnets,[4] or superconductors.[5] Furthermore, specific charge, spin, and orbital ordering phenomena give rise to a wide-ranging spectrum of physical responses. Structural variety is by no means a less relevant factor, to which the diversity of bulk properties of oxides can be related. For instance, antiferromagnetic exchange coupling of electron spins on a trigonal lattice is frustrated and raises a rich energy landscape of ordered magnetic states.[6] Upon removal of part of the spin bearing species from such a lattice (for example, by leaving behind a Kagomé-type pattern), frustrated magnetic exchange couplings may persist, while further breaking down the dimensionality leads to monomeric or oligomeric complex oxoanions, potentially behaving as single molecule magnets.[7] In particular, 2D trigonal lattices continue to be the focus of solid materials research, in combination with the phenomena of magnetic frustration and effects that are suited to lift the phenomenon.[6]

Herein, we report on a new oxoruthenate(V) featuring trigonal geometry. The potentially 2D trigonal spin lattice is broken down by interrupting the 2D exchange pathways after insertion of diamagnetic silver.

Single-phase β-Ag_3RuO_4 has been synthesized from Ag_2O and $KRuO_4$ as a coarse crystalline product (Figure 1a), using hydrothermal conditions. The shiny crystals are insensitive to water and air, and start to decompose at 400 °C, leaving metallic silver and RuO_2 as solid residues. β-Ag_3RuO_4 features an unprecedented crystal structure,[8] which can be regarded as a ternary, cation-ordered variant with a NiAs-type structure: oxygen replaces As in the NiAs structure, which consequently adopts a hexagonal close packed (hcp) motif wherein Ag and Ru occupy the octahedral voids in a fully ordered fashion. In accordance with its well-known inclination to adopt low coordination numbers, silver is shifted off the centers of the octahedral voids, resulting in first neighbor coordination numbers of two and three. In a structurally related sulfide, $LiCrS_2$,[9] alkali and transition metals segregate into trigonal slabs ($[LiS_{2/2}]$ and $[CrS_{2/2}]$) with the unpaired spins of d^3-configured chromium thus residing on a trigonal lattice. Likewise, the cations in β-Ag_3RuO_4 separate into layers corresponding to the formula $Ag(Ag_{1/2}Ru_{1/2})O_2 \equiv Ag_2[AgRuO_4]$, as displayed in Figure 1b. In this way the frustration of the antiferromagnetic exchange coupling on the trigonal sublattice hosting Ru^V is lifted. Interestingly, the ruthenium(V) atoms are not distributed homogeneously, but segregate into clusters of (Ru_4) diamonds that are separated by diamagnetic silver atoms. The resulting tetrameric polyoxoanions $[Ru_4O_{16}]^{12-}$, are the most promi-

---

[*] Dr. B. E. Prasad, Prof. P. Kazin, Dr. A. C. Komarek, Prof. Dr. C. Felser, Prof. Dr. M. Jansen
Max-Planck-Institut für Chemische Physik fester Stoffe
01187 Dresden (Germany)

Prof. Dr. M. Jansen
Max-Planck-Institut für Festkörperforschung
70569 Stuttgart (Germany)
E-mail: M.Jansen@fkf.mpg.de

Prof. P. Kazin
Department of Chemistry, Moscow State University
119991 Moscow (Russia)

Supporting information and the ORCID identification number(s) for the author(s) of this article can be found under http://dx.doi.org/10.1002/anie.201510576.

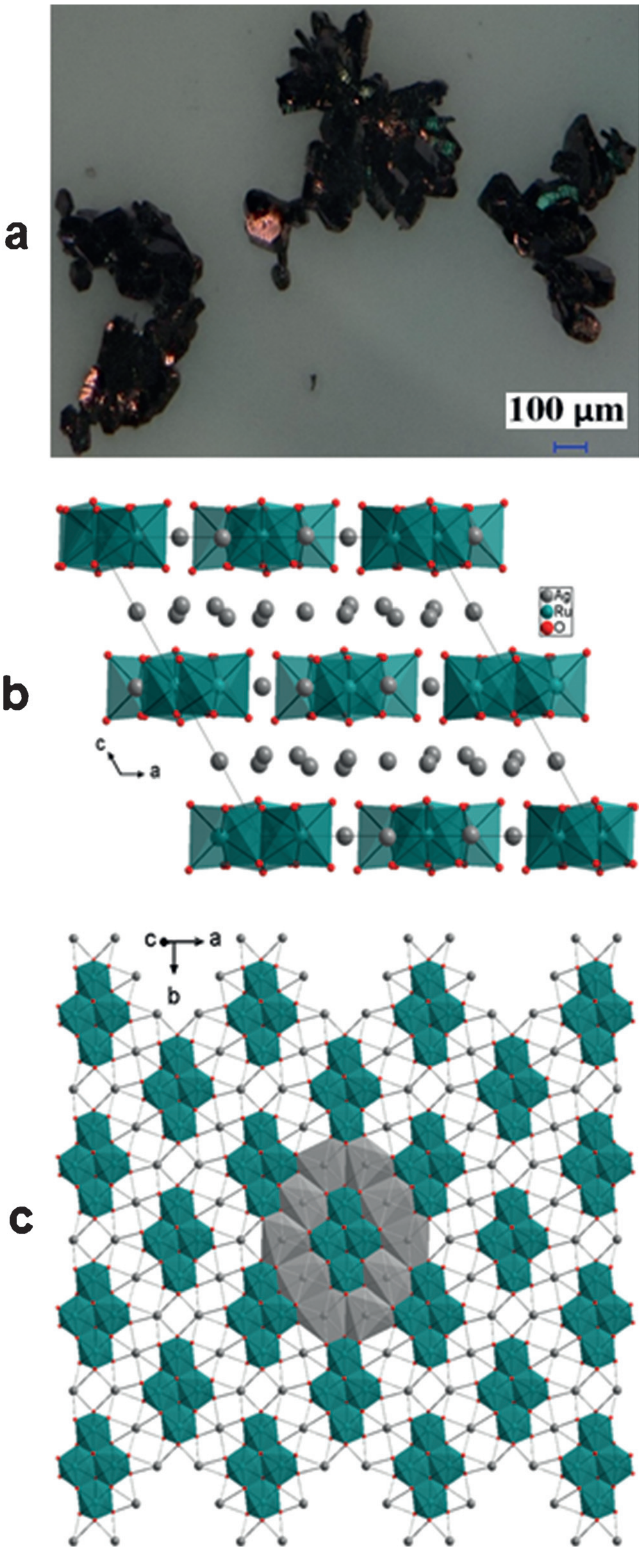

Figure 1. a) Light microscope image of β-Ag_3RuO_4 crystals. b) and c) Crystal structure of β-Ag_3RuO_4 viewed along different crystallographic axes. Gray polyhedra in (c) correspond to silver.

nent local structural constituent. As displayed in Figure 1 c, its structure consists of four RuO_6 octahedra, each sharing two edges in a *cis*-position with respect to neighboring octahedra. The bond lengths are in the range expected for Ru^{V}, and in accordance with variations in the functions of oxygen atoms within the crystal structure.

Previously reported α-Ag_3RuO_4 is based on a ccp arrangement of oxygen atoms and exhibits a polyanionic strand consisting of *cis*-edge linked RuO_6 octahedra.[10] Considering the tetrameric anion of β-Ag_3RuO_4, a ring structure, one may regard the two kinds of complex oxoanions as topologically equivalent.

The magnetic properties of the compound, represented as χ (magnetic susceptibility) and χT as a function of temperature in Figure 2, are quite unusual and reflect its cluster nature. Above 80 K, that is within the regime of paramagnetic response, χ is reversible (Figure 2, left scale) and is independent of the magnetic field applied (Supporting Information, Figure S1). The approximately linear part of $1/\chi(T)$, lying between 200 and 300 K, follows the Curie–Weiss equation with a μ_{eff} of 4.01 μ_B per Ru atom and θ -390 K (Figure 2, inset). This value corresponds fairly well to Ru^{5+} ions with $S = 3/2$ (theoretical $\mu_{\mathrm{eff}} = 3.87$ μ_B). Notably, the large negative θ indicates that strong intracluster antiferromagnetic exchange interactions prevail. Around 80 K a pronounced cusp in the susceptibility evolves, which becomes strongly dependent on field strength (Supporting Information, Figure S1), suggesting that a magnetic phase transition occurs.

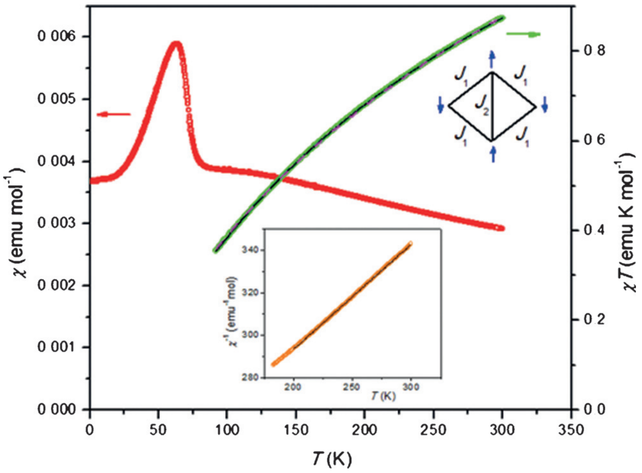

Figure 2. Temperature dependence of magnetic susceptibility χ (red), reciprocal susceptibility χ^{-1} (inset, orange), product χT (green) of β-Ag_3RuO_4 under a field of 50 kOe. Fits of χT (see text) with the constraint $J_2 = J_1$ (dashed magenta line), and without constraints (black line). Insert picture: rhomb of ruthenium tetramer, the spin orientation for the ground state is shown.

It is reasonable to assume that the strong magnetic exchange interaction is limited to $[Ru_4O_{16}]^{12-}$ tetramers, since the intercluster interactions will be substantially dampened by the surrounding Ag^{+} ions. Based on this premise, susceptibility in the range 90–300 K was analyzed using a Heisenberg model with four equal exchange integrals J_1 along every side of the rhomb, and a different J_2 and J_3 along the short and long diagonals, respectively (see Figure 2). The respective Hamiltonian is designated by Equation 1.

$$\hat{H} = -2J_2\hat{S}_1\hat{S}_2 - 2J_3\hat{S}_3\hat{S}_4 - 2J_1(\hat{S}_1\hat{S}_3 + \hat{S}_1\hat{S}_4 + \hat{S}_2\hat{S}_3 + \hat{S}_2\hat{S}_4) + \beta H[g_1(\hat{S}_1 + \hat{S}_2) + g_3(\hat{S}_3 + \hat{S}_4)] \quad (1)$$

On the basis of a reported[11] function, dependence ($\chi T(T)$) was fitted with $S_1 = S_2 = S_3 = S_4 = 3/2$ and $g_1 = g_3 = g$ (Supporting Information). Since the long diagonal is 5.39 Å in length, that is considerably longer than the other rhomb dimensions, J_3 was fixed to 0.

The fitting shows that susceptibility values are mostly determined by J_1, while J_2 only affects the data slightly. Although one would expect similar J_1 and J_2 values for geometric reasons, the best fit resulted in exchange parameters with opposite signs ($J_1 = -36.732(7)$ K, $J_2 = 28.3(1)$ K, $g = 1.9208(3)$ with $R^2 = 0.99999$). Exchange parameters with opposite signs may be sensible if different local coordination geometries of ruthenium atoms are considered. Possible competing ferro- and antiferromagnetic exchange contributions from different exchange channels may result in a positive J for one ruthenium pair and a negative J for the other. An alternate fitting with the constraint $J_2 = J_1$ gave $J_1 = -31.74(4)$ K, and $g = 2.0001(8)$, with an R^2 of 0.99976. Therefore we can only consider with confidence, the J_1 value lying between those values obtained using the first and second fit, while the J_2 value is not fully relevant.

The ground state of such a tetramer is a spin-singlet, with two spins down at the long diagonal and two spins up at the short diagonal (see Figure 2). Here we can see a frustration-like phenomenon. Although antiferromagnetic coupling between neighboring Ru^{5+} was expected, spins over the short diagonal happen to be aligned ferromagnetically because of an antiferromagnetic interaction with the other two ruthenium ions along the edges of the rhomb. Statistically, the latter interaction is thus twice as strong as the one across the short diagonal, thereby frustrating the expected antiferromagnetic coupling.

The susceptibility response below 80 K is peculiar. Field-cooled (FC) and zero-field-cooled (ZFC) curves almost coincide under a high field of 50 kOe. On cooling and after a sharp increase below 80 K, $\chi(T)$ exhibits a maximum at about 62–64 K and decreases back to a smaller value. Such behavior is unusual for an FC curve, which is expected to show monotonous growth with possible saturation at low temperatures. This experimental result is fully reproducible, as was demonstrated on two samples synthesized in different batches. The temperature dependence of the AC susceptibility, as well as the field dependence of magnetization at temperatures below the transition temperature, is shown in Figure 3. Under a zero DC field, both $\chi'(T)$ and $\chi''(T)$ exhibit a maximum at 69 K and do not depend on the AC frequency. With an increasing DC magnetic field, the $\chi'(T)$ peak shifts only slightly to higher temperatures (1–3 K). The $\chi''(T)$ peak fully disappears under a low field of 1 kOe, implying that magnetization becomes reversible under an AC field. Thus, there is no distinct sign of a magnetization relaxation behavior that usually characterizes a transition to a spin-glass state. Therefore, the features considered reflect the transition to a particular magnetically ordered state.

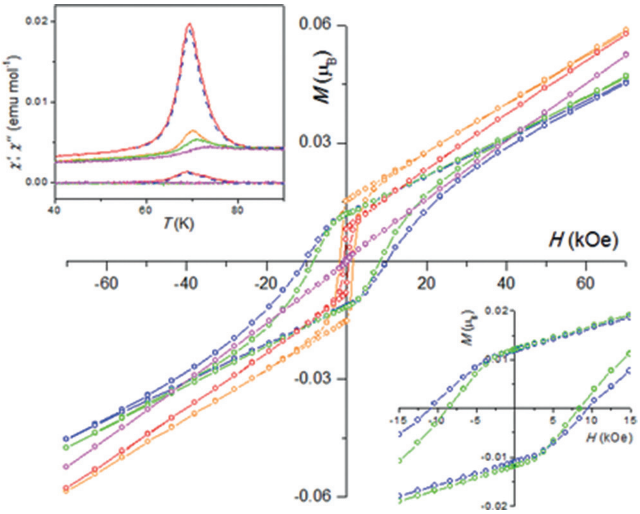

Figure 3. Magnetic properties of β-Ag_3RuO_4. Inset, top left: real (upper curves) and imaginary (lower curves) parts of magnetic susceptibility vs. temperature at an AC frequency of 80 Hz, and DC fields H = 0 (red), 1 kOe (orange), 10 kOe (green), 50 kOe (magenta), and at an AC frequency of 450 Hz and H = 0 (blue dashes). Main figure: hysteresis magnetization loops at temperatures $T = 1.8$ K (blue), 30 K (green), 62 K (orange), 69 K (red), 74 K (magenta). Inset, bottom right: parts of magnetization loops after field cooling under $H = 70$ kOe, showing a bias-effect; the bias value is defined as $H_{bs} = [H_c(\text{descending field}) - H_c(\text{ascending field})]/2$; at $T = 1.8$ K (blue), $H_{bs} = 0.72$ kOe; at $T = 30$ K (green), $H_{bs} = 0.12$ kOe.

The field dependence of magnetization below the transition temperature is of non-linear and hysteretic character. The coercivity (H_c) increases constantly with decreasing temperature, approaching 10 kOe at 1.8 K. The remanent magnetization (M_r) reaches a maximum value of 0.015 μ_B at 62 K, decreases to 0.012 μ_B at 30 K, and remains unchanged up to 1.8 K, constituting only a small part of the maximum value of 3 μ_B expected for ferromagnetically ordered Ru^{5+} ions.

At first glance, the weak ferromagnetism encountered appears to contradict our conclusion about strong antiferromagnetic interactions occurring between ruthenium tetramer anions, leading to a ground state with $S = 0$. A probable reason for the observed small non-compensated magnetic moment is the effect of spin-orbit coupling. Recent works suggest non-negligible orbital moment contribution to magnetism of octahedrally coordinated Ru^{5+}, in spite of its orbitally non-degenerate ground state $^4A_{2g}$.[12] In the centrosymmetric $[Ru_4O_{16}]$ unit in β-Ag_3RuO_4, a small misalignment angle between initially antiparallel directions of the diagonal spin-pairs may appear (allowed by symmetry) because of second order spin–orbit coupling, thereby forming a small residual magnetic moment. This provides weak spontaneous magnetization in the antiferromagnetic state below 80 K, which in fact represents a kind of spin-canted antiferromagnetism described by antisymmetric exchange interactions.[13] The fact that a plot of spontaneous magnetization versus temperature shows a cusp is also not surprising. A tiny change of geometry in the ruthenium tetramer with temperature may affect the proposed small misorientation angle considerably, so that the angle and the corresponding residual magnetic moment decrease with lowering temperature.

This type of canted spin magnetic order can also be considered as non-compensated antiferromagnetism, which was recently shown to provide very strong magnetic anisotropy and a giant magnetization bias effect.[14] To check the latter, we measured the magnetization loops after cooling the sample below the transition temperature under a field of 70 kOe (Figure 3, bottom right inset). A small but distinct hysteresis bias was observed at 1.8 and 30 K, suggesting that the magnetic anisotropy field value exceeds 70 kOe at these temperatures.

In conclusion, a new oxoruthenate(V) complex featuring an unprecedented tetrameric complex oxoanion $[Ru_4O_{16}]^{12-}$ embedded in a 2D trigonal slab MO_2 was presented. The magnetic studies suggest that strongly antiferromagnetically interacting spins within the $[Ru_4O_{16}]^{12-}$ ion result in a formally spin-singlet ground state. Part of the characteristic frustration of antiferromagnetic exchange coupling on trigonal spin lattices persists, even in the tetramer, but is overcome because only one out of five relevant antiferromagnetic intracluster exchange paths is frustrated. Furthermore, we suggest that the formal spin-singlet ground state develops a small net magnetic moment because of second order spin-orbit coupling, and that the magnetic ordering of these net moments at low temperature provides the observed weak ferromagnetism with high magnetic anisotropy. The strong magnetic anisotropy of the $[Ru_4O_{16}]^{12-}$ ion, as well as the effectively orbital nature of its net magnetic moment, suggests that this anion may reveal the properties of a single-molecule magnet if well-diluted in a diamagnetic matrix.

Experimental Section

Synthesis: The title compound was synthesized from Ag_2O (freshly precipitated from an aqueous solution of $AgNO_3$ with KOH) and $KRuO_4$ (Alfa Aesar 97%) by applying hydrothermal conditions using a Teflon-lined stainless steel autoclave. For a typical batch Ag_2O and $KRuO_4$ (400 mg, 3:2) were added to deionized water (8 mL). Subsequently, the mixture was stirred for 10–15 minutes before placement in a 25 mL autoclave and heating to 190–200 °C for 48–72 h. After switching off the heating source the autoclave was allowed to cool to room temperature. The product formed was removed by filtration, washed with deionized water and ethanol, and finally dried in a desiccator.

Thermal analysis: The thermal stability of the title compound was studied by TGA/DTA (NETZSCH STA 449 C, argon atmosphere, heating rate 10 K min^{-1}). The compound started to decompose at 400 °C. The weight loss (6.46%) observed during the first step of decomposition corresponds to the mass of two equivalents of oxygen. The decomposed product was characterized by PXRD and consists of metallic silver and RuO_2. The decomposition reaction may thus be represented by Equation 2.

$$Ag_3RuO_4 = 3\,Ag + RuO_2 + O_2 \qquad (2)$$

Acknowledgements

We thank H. Guo for assistance with the crystal structure analysis.

Keywords: antiferromagnetism · hydrothermal synthesis · magnetic anisotropy · oxoruthenates · trigonal spin lattices

How to cite: *Angew. Chem. Int. Ed.* **2016**, *55*, 4467–4471
Angew. Chem. **2016**, *128*, 4543–4547

[1] A. Bussmann-Holder, *J. Phys. Condens. Matter* **2012**, *24*, 273202 (29pp).

[2] a) W. Hesse, M. Jansen, W. Schnick, *Prog. Solid State Chem.* **1989**, *19*, 47–110; b) M. Jansen, H. Nuss, *Z. Anorg. Allg. Chem.* **2007**, *633*, 1307–1315; c) J. Winterlik, G. H. Fecher, C. A. Jenkins, C. Felser, C. Mühle, K. Doll, M. Jansen, L. M. Sandratskii, J. Kübler, *Phys. Rev. Lett.* **2009**, *102*, 016401.

[3] a) A. von Hippel, *Rev. Mod. Phys.* **1950**, *22*, 221–237; b) H. Ito, Y. Shiozaki, E. Sawaguchi, *J. Phys. Soc. Jpn.* **1983**, *52*, 913–919; c) X. H. Wang, I. W. Chen, X. Y. Deng, Y. O. Wang, L. T. Li, *J. Adv. Ceram.* **2015**, *4*, 1–21.

[4] a) J. Philip, A. Punnoose, B. I. Kim, K. M. Reddy, S. Layne, J. O. Holmes, B. Satpati, P. R. Leclair, T. S. Santos, S. Moodera, *Nat. Mater.* **2006**, *5*, 298–304; b) A. Sundaresan, R. Bhargavi, N. Rangarajan, U. Siddesh, C. N. R. Rao, *Phys. Rev. B* **2006**, *74*, 161306.

[5] a) S. N. Putilin, E. Antipov, O. Chmaissem, M. Marezio, *Nature* **1993**, *362*, 226–228; b) A. Schilling, M. Cantoni, J. D. Guo, H. R. Ott, *Nature* **1993**, *363*, 56–58; c) C. W. Chu, L. Gao, F. Chen, Z. J. Huang, R. L. Meng, Y. Y. Xue, *Nature* **1993**, *365*, 323–325.

[6] a) M. F. Collins, O. A. Petrenko, *Can. J. Phys.* **1997**, *75*, 605–655; b) A. P. Ramirez, *Annu. Rev. Mater. Sci.* **1994**, *24*, 453–480; c) A. I. Coldea, L. Seabra, A. McCollam, A. Carrington, L. Malone, A. F. Bangura, D. Vignolles, P. G. van Rhee, R. D. McDonald, T. Sörgel, M. Jansen, N. Shannon, R. Coldea, *Phys. Rev. B* **2014**, *90*, 020401; d) Y. Drees, D. Lamago, A. Piovano, A. C. Komarek, *Nat. Commun.* **2013**, *4*, 2449; e) Y. Drees, Z. W. Li, A. Ricci, M. Rotter, W. Schmidt, D. Lamago, O. Sobolev, U. Rütt, O. Gutowski, M. Sprung, A. Piovano, J. P. Castellan, A. C. Komarek, *Nat. Commun.* **2014**, *5*, 5731.

[7] a) N. Stüßer, M. Sofin, R. Bircher, H.-U. Güdel, M. Jansen, *Chem. Eur. J.* **2006**, *12*, 5452–5457; b) A. Jesche, R. W. McCallum, S. Thimmaiah, J. L. Jacobs, V. Taufour, A. Kreyssig, R. S. Houk, S. L. BuO'ko, P. C. Canfield, *Nat. Commun.* **2014**, *5*, 3333; c) P. E. Kazin, M. A. Zykin, W. Schnelle, C. Felser, M. Jansen, *Chem. Commun.* **2014**, *50*, 9325–9328.

[8] Crystal data of Ag_3RuO_4: monoclinic, space group *C*2/*c* (No.15), $a = 1354.42(5)$ pm, $b = 1124.27(3)$ pm, $c = 1279.33(4)$ pm, $\beta = 120.9425(2)°$, $V = 1670.84(9) \times 10^6$ pm^3,$\rho_{calcd} = 7.7712$ g cm^{-3}, $Z = 16$, $\mu Mo_{K\alpha} = 17.285$ mm^{-1}, $F(000) = 3472$, $\lambda = 71.069$ pm, Bruker D8 VENTURE X-ray diffractometer, bent graphite monochromator, $T = 293$ K, ω-/ϕ-scan, 3137 measured reflections, 1522 symmetry independent reflections ($2\theta_{max} = 50°$), 150 refined parameters. Multi-scan absorption correction program (SADABS) was used. The structure solution and refinement have been performed using Jana2006:[15] $R = 0.0333$ and $wR2 = 0.0787$. Twinning matrix: (1 0 −1, 0, 1, 0, 0, 0, −1); with twin fractions (50.1 (2)%:49.9(2)%). Further details on the crystal structure investigations may be obtained from the Fachinformationszentrum Karlsruhe, 76344 Eggenstein-Leopoldshafen, Germany (fax: (+49) 7247-808-666; e-mail: crysdata@fiz-karlsruhe.de), on quoting the depository number CSD-430440.

[9] a) J. R. Dahn, W. R. McKinnon, R. R. Haering, W. J. L. Buyers, B. M. Powell, *Can. J. Phys.* **1980**, *58*, 207–213; b) J. G. White,

H. L. Pinch, *Inorg. Chem.* **1970**, *9*, 2581 – 2583; c) B. van Laar, D. J. W. Ijdo, *J. Solid State Chem.* **1971**, *3*, 590 – 595.
[10] W. Klein, M. Jansen, *Acta Crystallogr. Sect. C* **2005**, *61*, i1 – i2.
[11] G. A. Kakos, G. Winter, *Aust. J. Chem.* **1969**, *22*, 97 – 107.
[12] a) S. G. Ebbinghaus, E. W. Scheidt, T. Götzfried, *Phys. Rev. B* **2007**, *75*, 144414; b) T. Götzfried, A. Reller, S. G. Ebbinghaus, *Solid State Sci.* **2004**, *6*, 1205 – 1210; c) T. Götzfried, A. Reller, S. G. Ebbinghaus, *Inorg. Chem.* **2005**, *44*, 6550 – 6557.
[13] R. L. Carlin *Magnetochemistry*, Springer, Berlin, **1986**.
[14] A. K. Nayak, M. Nicklas, S. Chadov, P. Khuntia, C. Shekhar, A. Kalache, M. Baenitz, Y. Skourski, V. K. Guduru, A. Puri, U. Zeitler, J. M. D. Coey, C. Felser, *Nat. Mater.* **2015**, *14*, 679 – 684.
[15] a) V. Petricek, M. Dusek, L. Palatinus, Jana 2006, Structure Determination Software Programs, Institute of Physics, Praha, Czech Republic, **2006**; b) L. Palatinus, G. Chapuis, *J. Appl. Crystallogr.* **2007**, *40*, 786 – 790.

Received: November 15, 2015